Journal of Geophysical Research - Solid Earth

Supporting Information for

Transpressional Rupture Cascade of the 2016 M_w 7.8 Kaikoura Earthquake, New Zealand

Wenbin Xu[1*], Guangcai Feng[2*], Lingsen Meng[3*], Ailin Zhang[3], Jean Paul Ampuero[4], Roland Bürgmann[5], Lihua Fang[6]

1Department of Land Surveying and Geo-informatics, Hong Kong Polytechnic University, China

2School of Geosciences and Info-Physics, Central South University, Changsha 410083, Hunan, China

3Department of Earth Planetary and Space Sciences, University of California, Los Angeles, CA 90025, USA

4Seismological Laboratory, California Institute of Technology, 1200 E. California Blvd., Pasadena, California 91125, USA

5Department of Earth and Planetary Science, University of California, Berkeley, California, USA

6Institute of Geophysics, China Earthquake Administration, Beijing 100081, China

*e-mail: wenbin.xu@polyu.edu.hk; fredgps@csu.edu.cn; meng@epss.ucla.edu

Contents of this file

Figures S1 to S13
Tables S1 to S3

Introduction

This document contains supplementary figures and tables. Figures S1 shows a subset of China Array stations. Figure S2 shows back projections of aftershocks at different depths. Figure S3 shows synthetic rupture scenarios of varying focal mechanisms. Figure S4-S7 show the coseismic InSAR data. Figure S8 shows the three dimensional surface displacement field. Figure S9 shows the difference between the coastal uplift lidar data (Clark et al., 2017) and the vertical displacement. Figure S10- S11 show the resolvability of InSAR data on the upper crustal faults and the Hikurangi subduction thrust, respectively. Figure S12 shows the complete GPS data and modeling results based on model I and model II. Figure S13 shows the checkerboard test for slip on the Point Kean fault of model III. Table S1 contains the SAR data used in the study. Table S2 summarizes the data used in modeling. Table S3 shows the comparison between estimated dip and rake angles and the fault database.

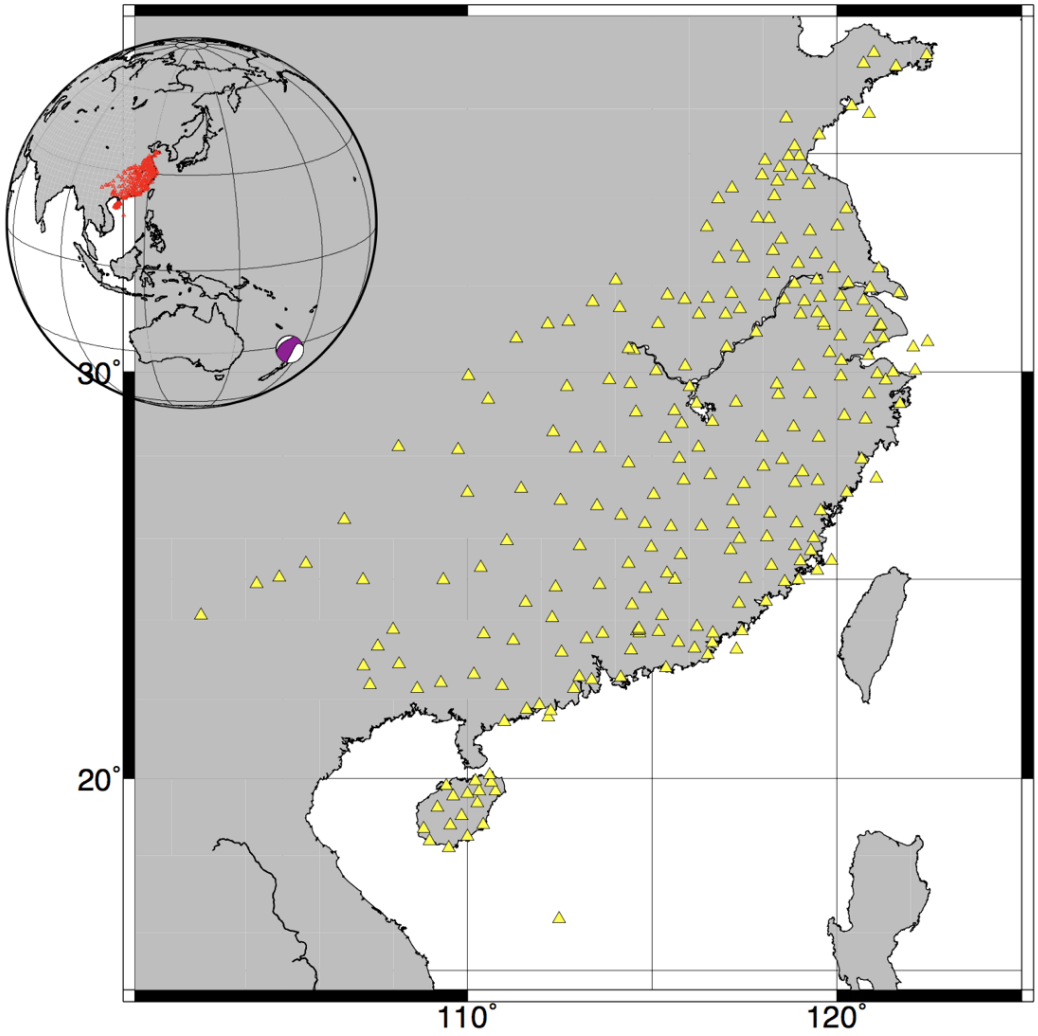

Figure S1 A subset of China Array stations involved in the back-projection analysis.

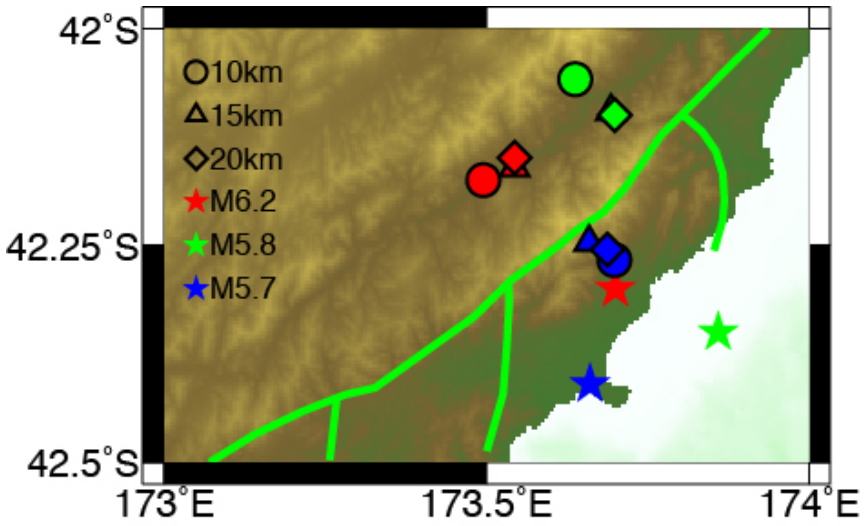

Figure S2 Back projections of aftershocks assuming different depths. Stars indicate the catalogue locations of the events. Colors denote events and symbols represent focal depths assumed in the BP. We back-project aftershock data at 10 km, 15 km, and 20 km and compare the obtained horizontal locations. We find that the location variation due to depth uncertainty is a minor factor compared with the spatial biases due to path effect.

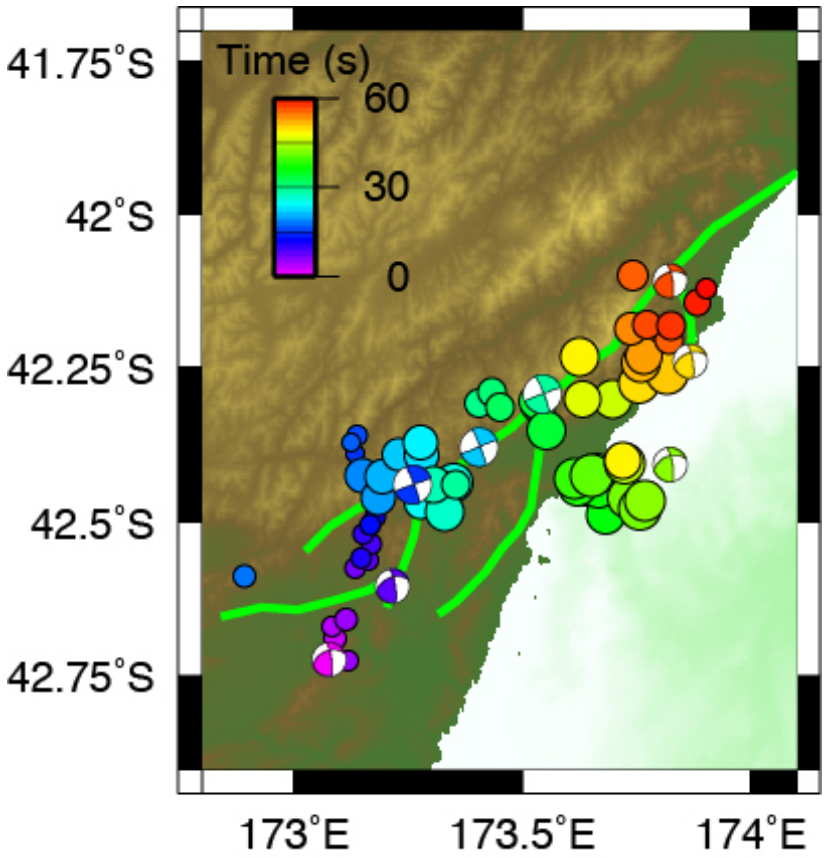

Figure S3 Synthetic rupture scenarios of varying focal mechanisms. BP radiators (circles) are sized by power and color-coded by time. Beach balls are also color-coded by time. Each beach ball indicates the corresponding mechanisms of eGF for each particular input subsource.

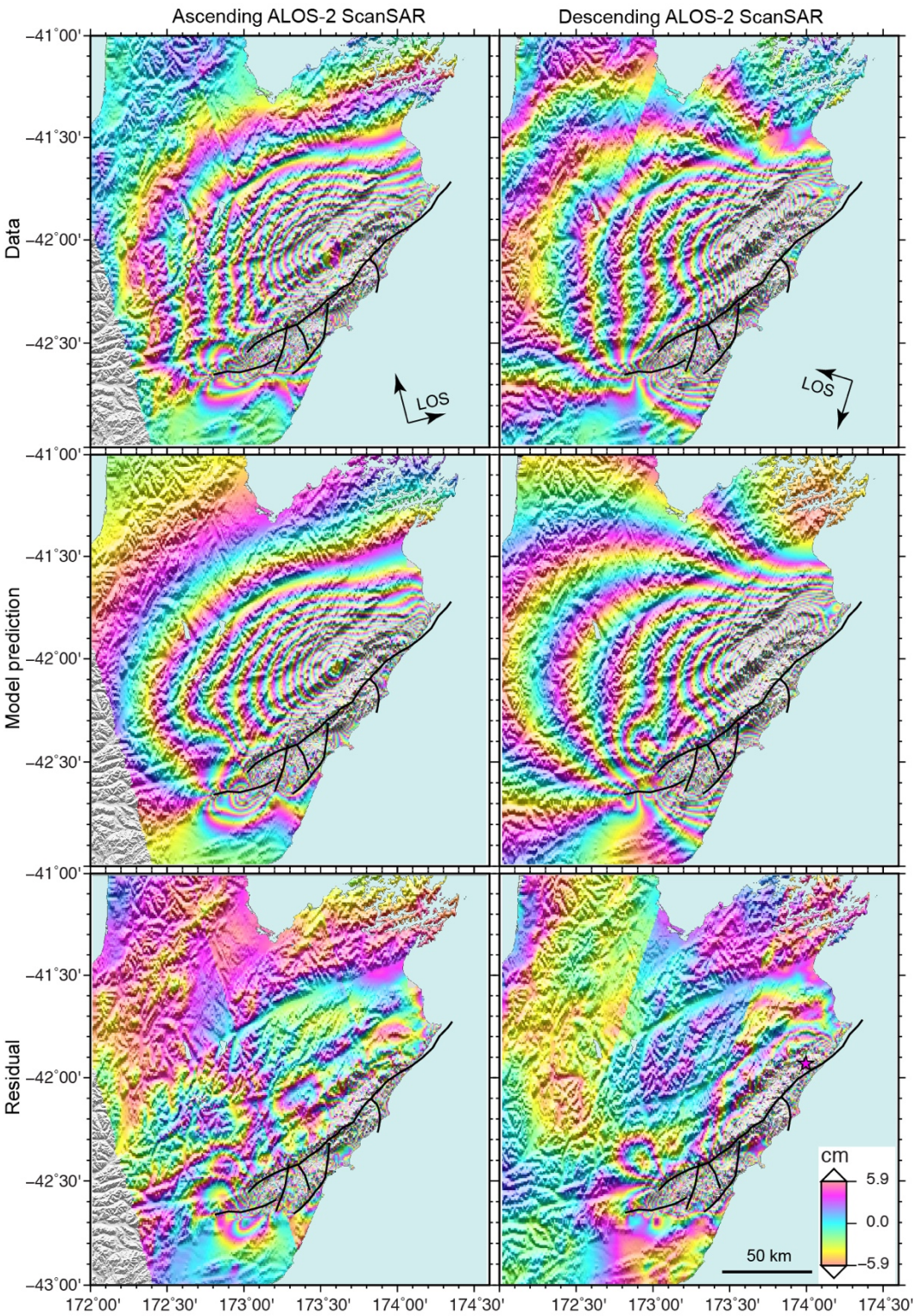

Figure S4 Coseismic ALOS-2 data of the 2016 Kaikoura earthquake and the modelling result. First row: Observed line-of-sight (LOS) displacement map. Middle row: Model I prediction. Last row: Residual. The black lines represent the fault geometry used in the modelling. Color scale is the same for all subpanels.

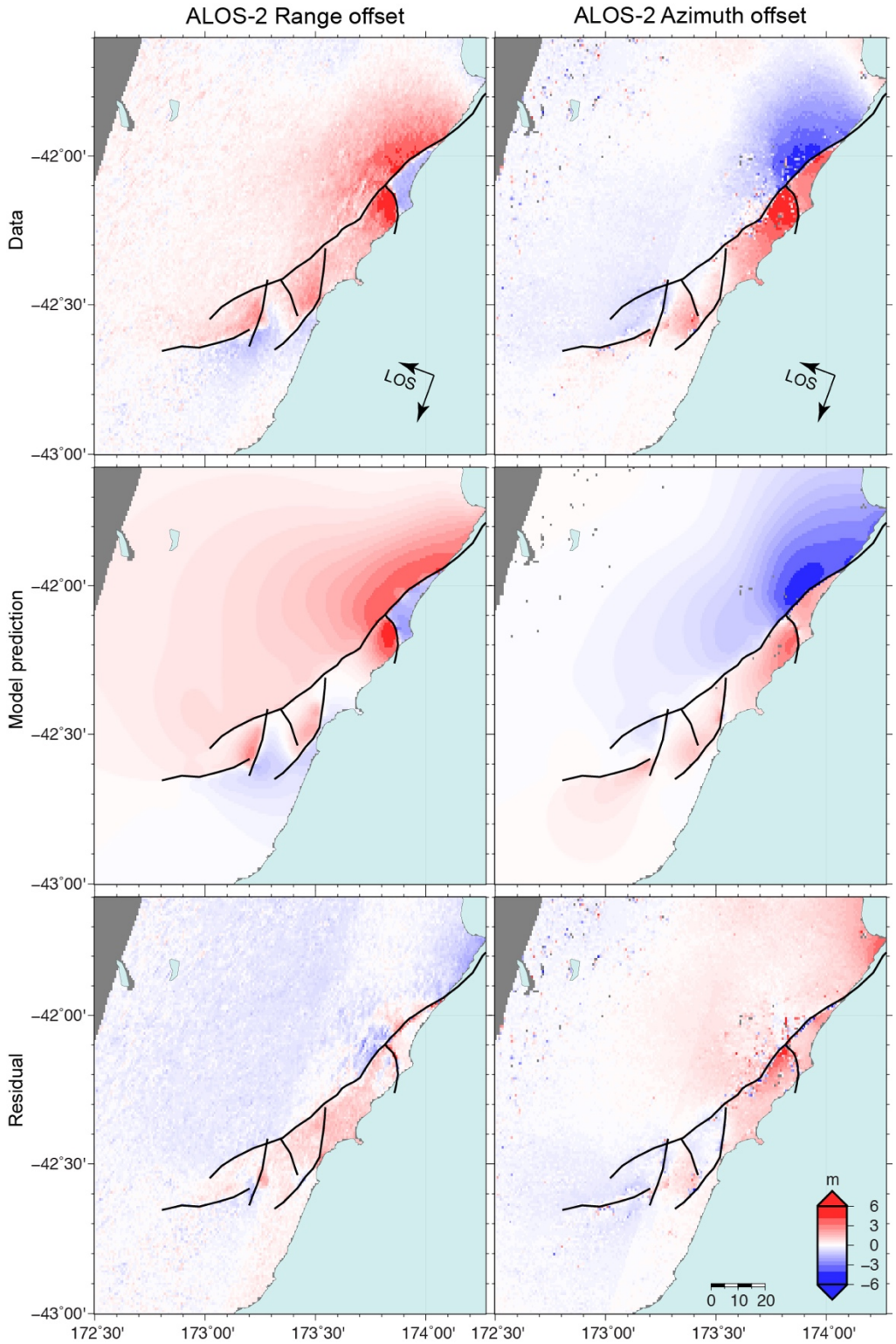

Figure S5 Coseismic descending ALOS-2 offsets of the 2016 Kaikoura earthquake and the modelling result. Range offsets are shown in the left column and azimuth offsets shown in right column. Negative range-offset values indicate the ground motion away from the satellite. Positive azimuth-offset values indicate the ground motion along the flight direction of the satellite. The same color scale is used for all subpanels.

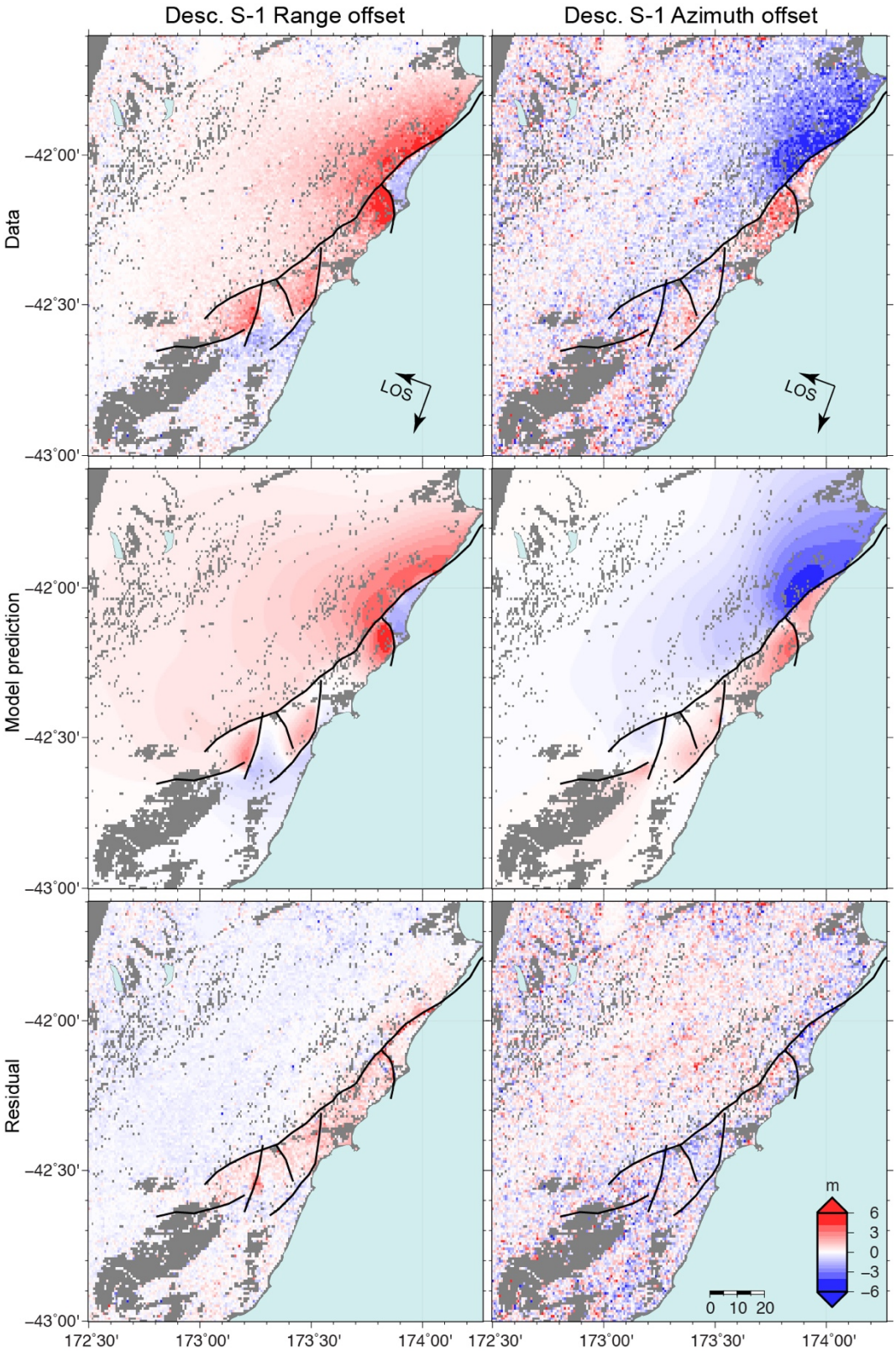

Figure S6 Same as Fig. S5 but for the descending Sentinel-1 offsets.

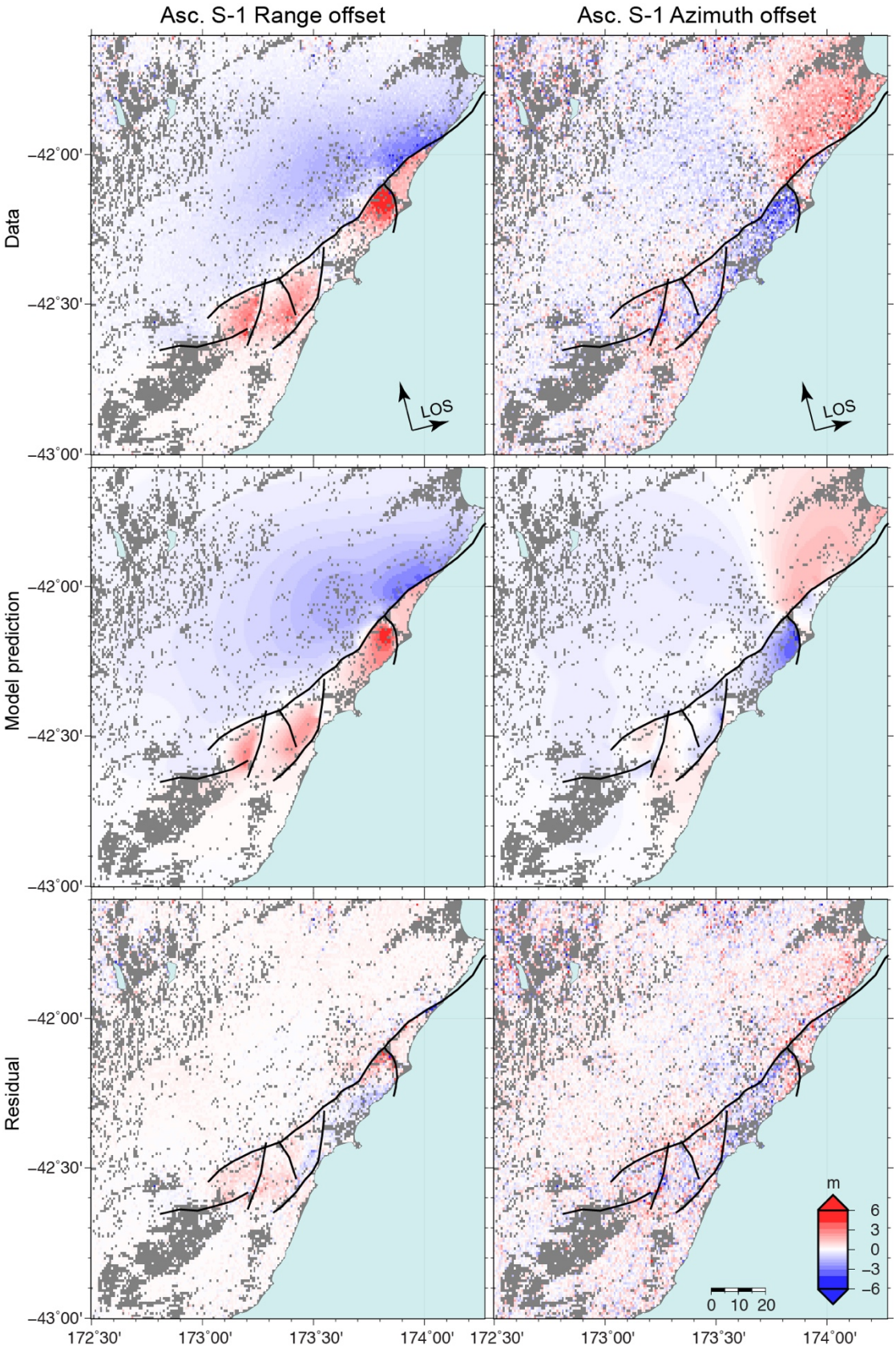

Figure S7 Same as Fig. S5 but for the ascending Sentinel-1 offsets.

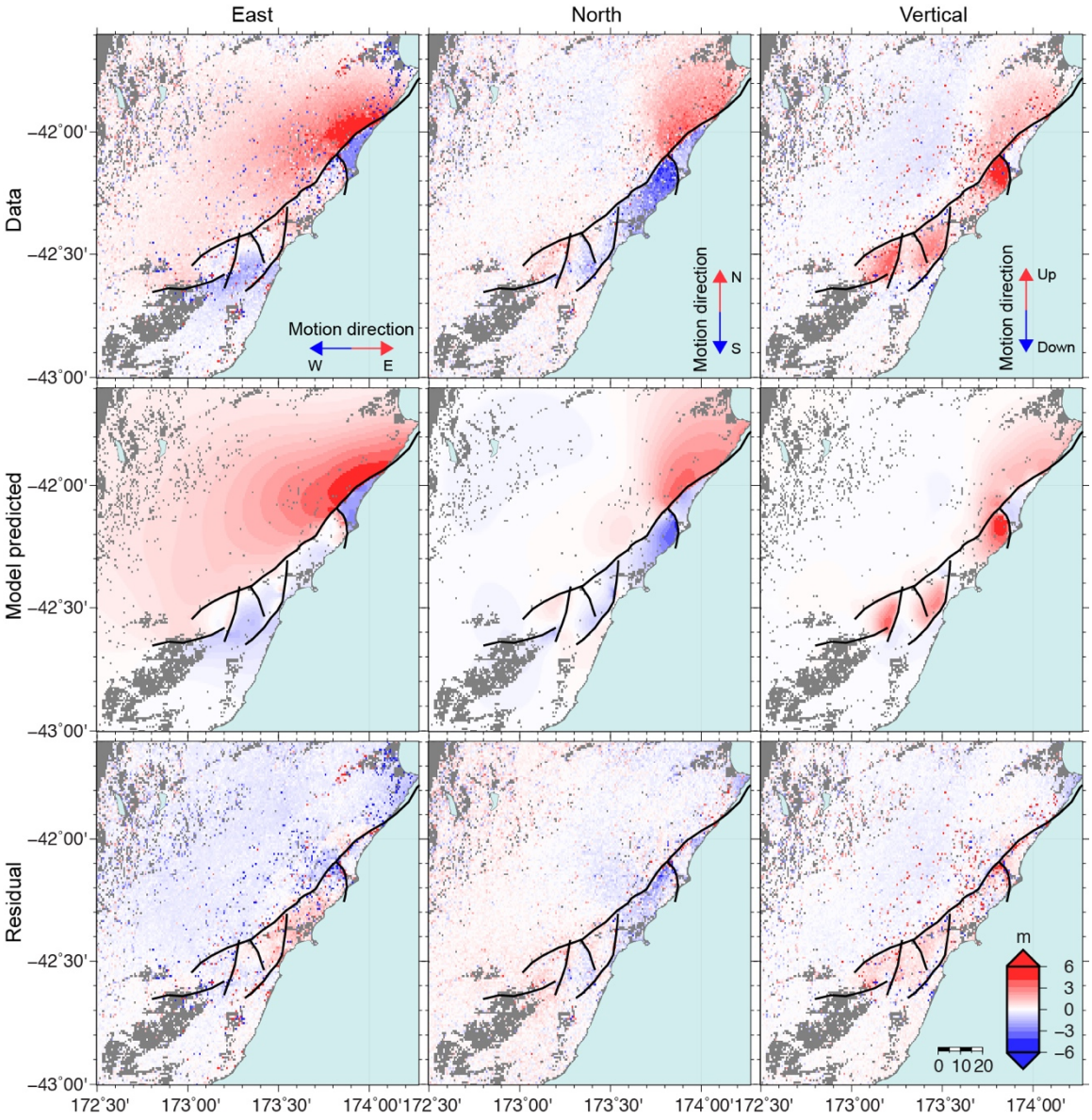

Figure S8 Three dimensional surface displacement field derived from image offsets of the Sentinel-1 and ALOS-2 data (first row). Model I predictions (second row). Residuals (last row).

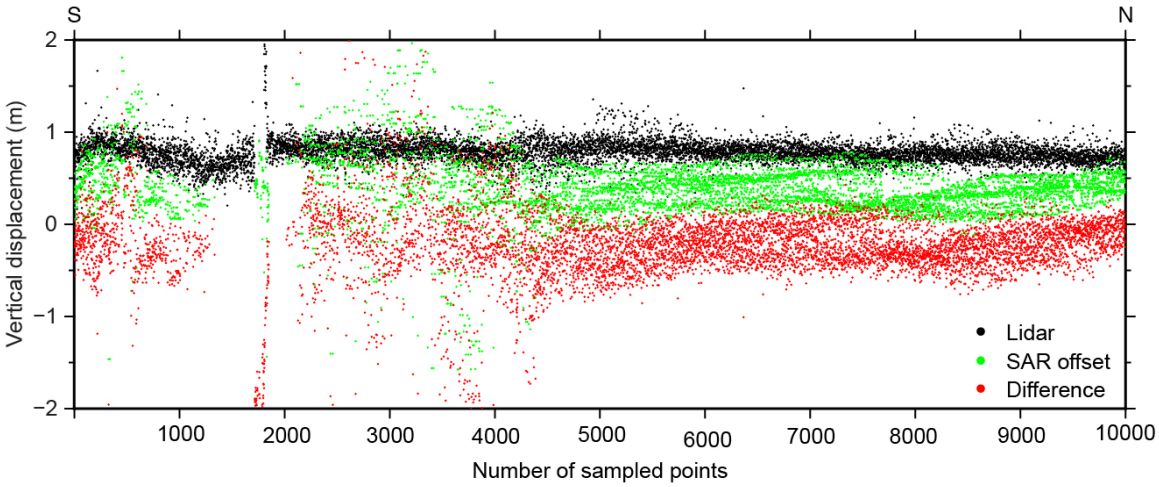

Figure S9 The comparison between the downsampled coastal uplift lidar data (Clark et al., 2017) and our vertical displacement. The systematic difference of ~0.4 cm between these two types of data is probably related to their spatial resolution difference and accuracy.

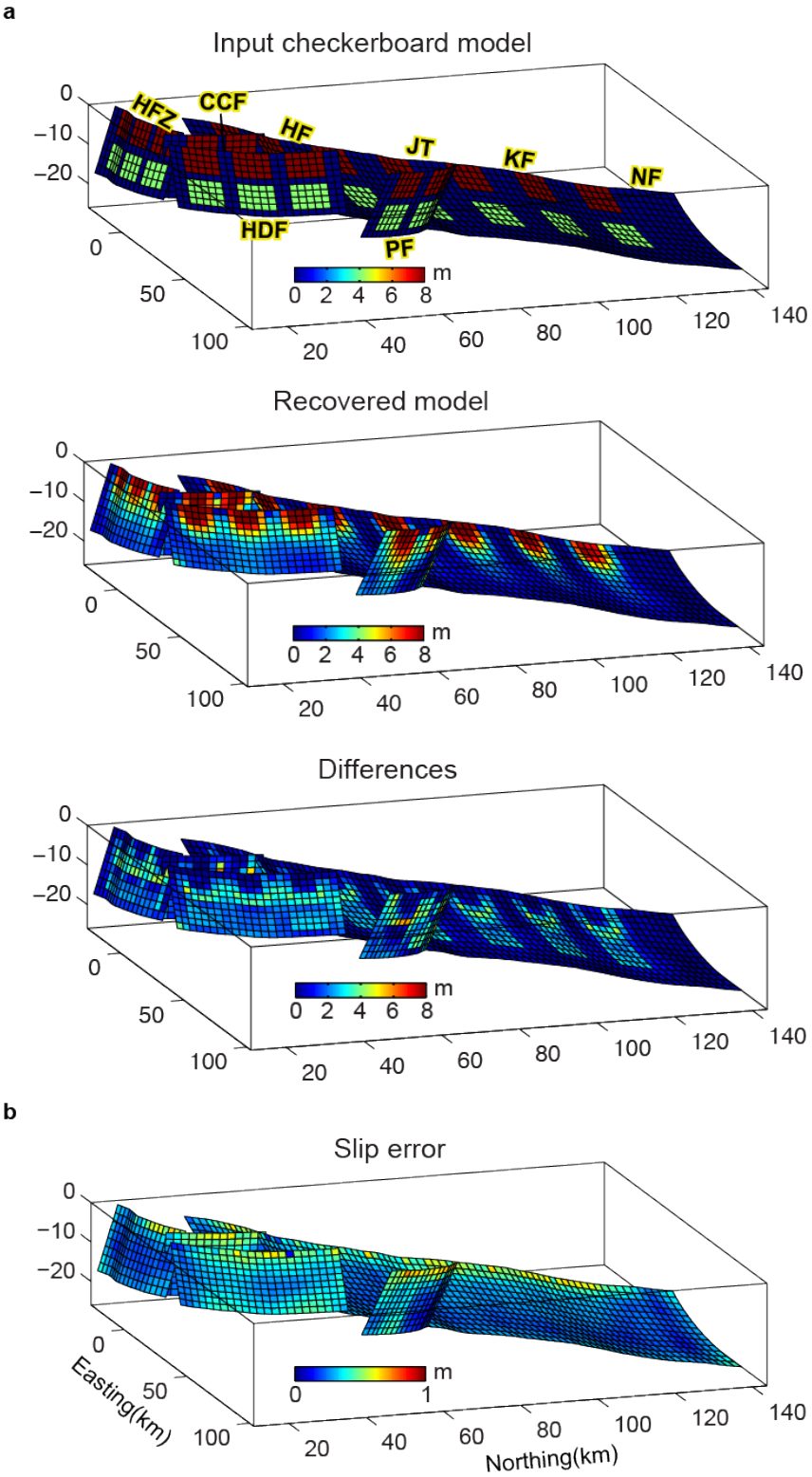

Figure S10 (a). The checkerboard test of model I. The result demonstrates that InSAR data have a very good resolvability for shallow fault slip, but poorer resolvability for deep slip. (b). Slip error estimated from 100 perturbed datasets generated using the Monte Carlo method.

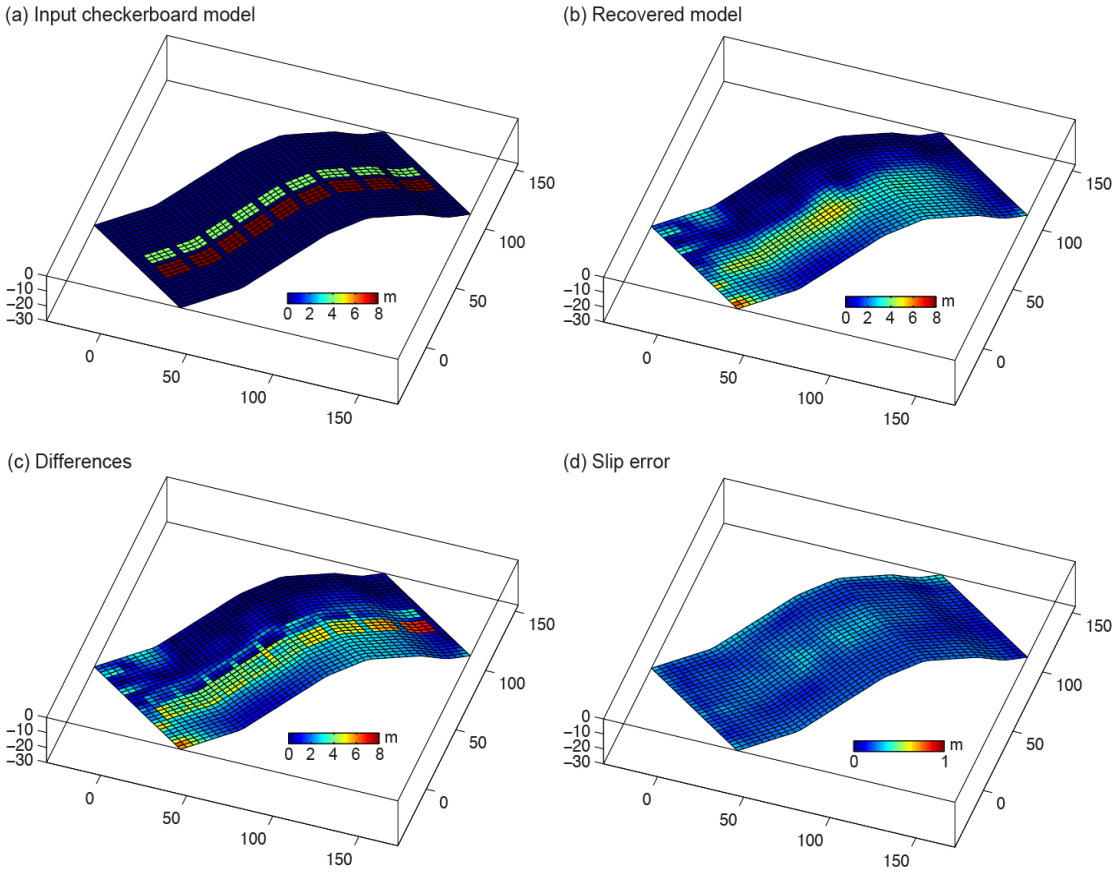

Figure S11 (a). The checkerboard test for slip on Hikurangi subduction thrust of model II. The results (b), (c) demonstrate that InSAR data have a poor resolution for deep slip on the subduction thrust. (d). Slip error estimated from 100 perturbed datasets generated using the Monte Carlo method.

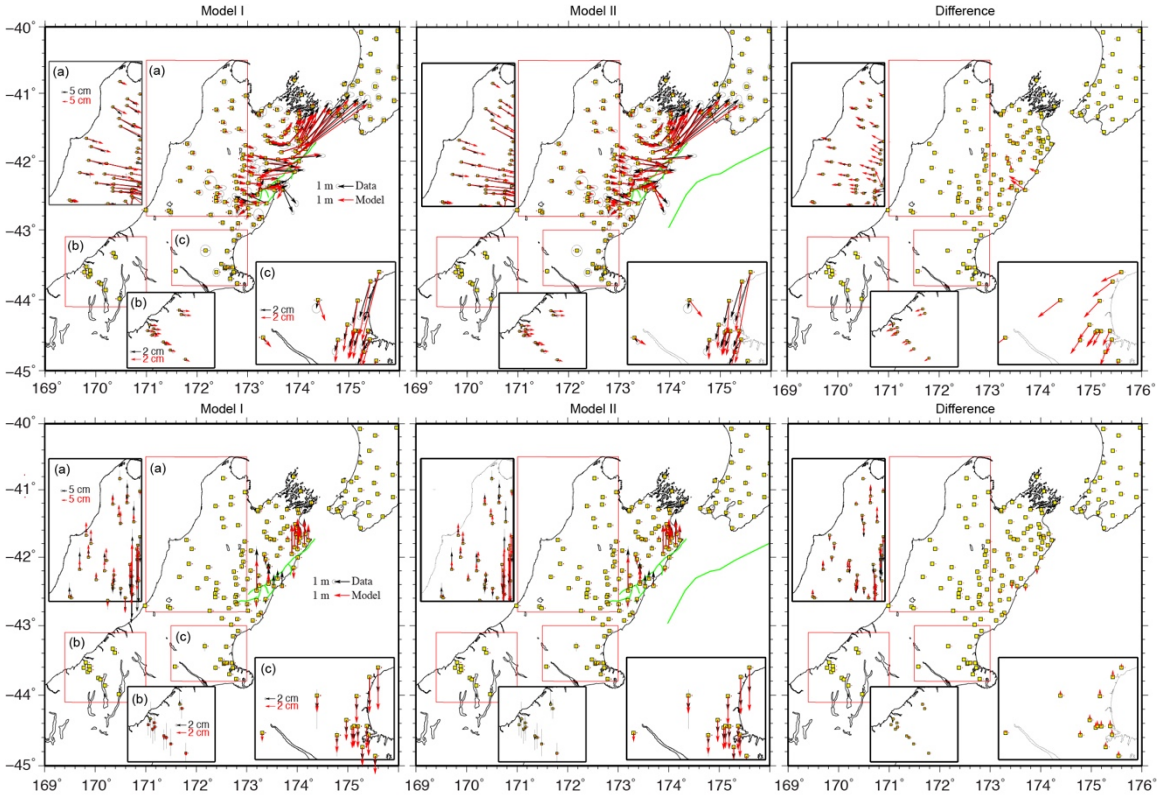

Figure S12 The complete coseismic GPS data (black) of the 2016 Kaikoura earthquake and the modelling result (red). The first and second row showing the horizontal and vertical GPS displacements, respectively.

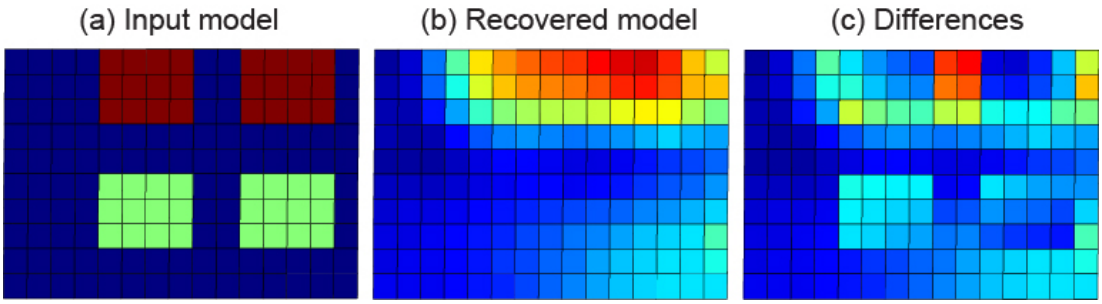

Figure S13 Same as Fig. S10 but for the checkerboard test for slip on the Point Kean fault of model III. The results (b), (c) demonstrate that InSAR data have a poor resolution for slip on the offshore Point Kean fault.

Table S1 SAR images used in this study

Sensor	Path	Master date (yyyy/mm/dd)	Slave date (yyyy/mm/dd)	Before (days)	After (days)	Perp. Baseline (m)	Orbit
ALOS-2	195	2016/10/23	2016/12/04	21	20	-150	Desc.
ALOS-2	102	2016/08/11	2016/12/01	91	17	130	Asc.
Sentinel-1	73	2016/09/15	2016/11/16	58	2	-10	Desc.
Sentinel-1	52	2016/11/03	2016/11/15	11	1	-10	Asc.

Table S2 Dataset used in generating three dimensional surface displacement and modeling

Data set	Reduced data points	Uncertainty (m^2)
Des. ALOS-2	4572	0.04
Asc. ALOS-2	5135	0.04
Des. ALOS-2 Azo	1108	0.43
Des. ALOS-2 Rng	691	0.28
Des. S-1 Azo	428	1.21
Des. S-1 Rng	927	0.81
Asc. S-1 Azo	420	0.85
Asc. S-1 Rng	1137	0.37

Table S3 Comparison with dip and rake angles from the fault database (Litchfield et al., 2014) and this study

Fault	Database		This study, model I	
	Dip [min, max], Best	Rake [min, max], Best	Dip [min, max], Best	Rake [min, max], Best
Hope Conway	[60, 80], 70	[169, 176], 173	70	[150, 172], 162
Jordan	[28, 48], 37	[90, 110], 100	[30, 50]	[145, 161], 153
Kekerengu 1	[50, 70], 60	[125, 145], 135	50	[141, 160], 151
Kekerengu 2	[70, 90], 80	[143, 163], 153	50	[150, 172], 160
Needles	[70, 90], 80	[147, 167], 157	[30, 50]	[150, 172], 160
Hope-Jordan Thrust-Kekerengu-Needles	[28, 90]	[90, 176], 144	[30, 50]	[130, 174], 158
Hundalee	[40, 70], 55	[90, 94], 90	50	[64, 90], 75